opening polymerization of Lys(Z)–NCA to obtain PEG–PBLA–PLys(Z) (Fig. 1). Different solvents were used for the syntheses of PEG–PBLA with varying degree of polymerization (DP). For example, PEG–PBLA (DP of PBLA=14) was prepared as follows: BLA–NCA (25 eq to the terminal primary amino group of PEG–NH_2) in DMF was added to PEG–NH_2 in DMF under an argon atmosphere, and stirred at 35°C for 20 h. After confirming the end of the polymerization from the disappearance of specific peaks of NCA in the IR spectrum (IR Report-100 spectrometer (JASCO, Tokyo, Japan)), the solution was poured into a mixture of *n*-hexane and ethyl acetate (6:4) to precipitate PEG–PBLA, and the precipitate was filtered and dried *in vacuo*. A series of PEG–PBLA with longer PBLA segments was prepared by a similar protocol with necessary changes in reaction conditions, including molar feed ratios of PEG–NH_2 to BLA–NCA, solvents and reaction times, as summarized in Table I. The obtained PEG–PBLAs were subsequently used for the ring-opening polymerization of Lys(Z)–NCA. Lys(Z)–NCA (50 eq to terminal primary amino group of PEG–PBLA) in a mixture of DMF and dichloromethane was added to PEG–PBLA in dichloromethane (final molar ratio of DMF to dichloromethane=1:10) under an argon atmosphere, and stirred at 35°C for 40 h. After confirming the end of the polymerization as in the case of the polymerization of BLA–NCA, the solution was poured into the 6:4 mixture of *n*-hexane and ethyl acetate to precipitate PEG–PBLA–PLys (Z), and the precipitate was filtered and dried *in vacuo*. Then, acetylation of the amino group of the N-terminal of PEG–PBLA–PLys(Z) was performed using acetic anhydride (3 eq to the terminal amino group of PEG–PBLA–PLys(Z)) in dichloromethane solution.

For estimation of the DP and molecular weight distribution (Mw/Mn) of the obtained PEG–PBLA–PLys(Z), a gel permeation chromatography (GPC) measurement was carried out using a TOSOH HLC-8220 equipped with TSKgel columns (Super AW4000 and Super AW3000X2), and an internal refractive index (RI) detector. NMP with 50 mM LiBr was used as an eluent at a flow rate of 0.3 ml min^{-1} at 40°C.

Preparation of PEG–PAsp(DET)–PLys Triblock Copolymer

Introduction of 1,2-diaminoethane units into the side chain of the PBLA segment in PEG–PBLA–PLys(Z) was performed by aminolysis reaction with excess of DET molecules (13), followed by the deprotection of the Z group with HBr/AcOH (Fig. 1). The typical synthetic procedure of PEG–PAsp(DET)–PLys with DP of PAsp(DET)=36 and PLys=50 was as follows: Three hundred milligram of PEG–PBLA–PLys(Z) (9.2 μmol) was lyophilized from benzene

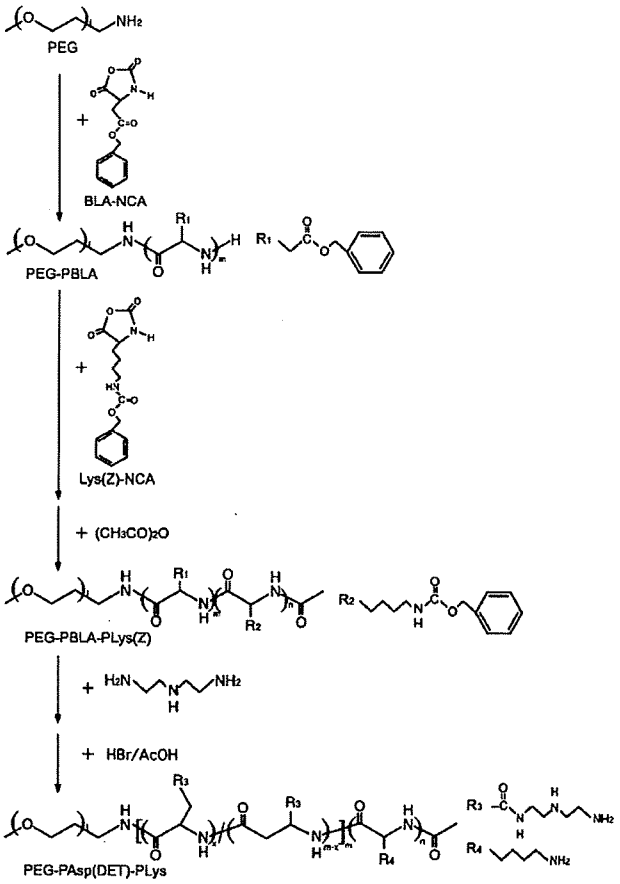

Fig. 1. Synthetic procedure of triblock copolymer, PEG–PAsp (DET)–PLys.

solution and dissolved into 6 mL of DMF. DET (1.8 mL, 16.7 mmol, 50 eq to benzyl groups of PBLA) was added under an argon atmosphere, and stirred at 40°C for 24 h. The mixture was dropped into diethyl ether (80 mL) with stirring, and then the white precipitate was filtered and redissolved in trifluoroacetic acid (2 mL). To deprotect the Z group, HBr (30% in acetic acid) was then added and stirred for 1 h, after which the solution was dropped into diethyl ether (40 mL) with stirring, and the resulting precipitate was purified by filtration and dried *in vacuo*. The crude product was dissolved in distilled water, dialyzed against 0.01 N HCl and then distilled water, and lyophilized to obtain the final product, PEG–PAsp(DET)–PLys as a hydrochloride salt form. The introduction of 1,2-diaminoethane units into the side chain of PAsp and the deprotection of Z group from the PLys(Z) segment were confirmed by ^1H NMR measurement (D_2O,

Table I. Reaction Condition and Composition of PEG–PBLA–PLys(Z)

Code	Molar feed ratio (PEG:BLA:Lys(Z))	Solvent/reaction time (h) for BLA polymerization	Solvent/reaction time (h) for Lys(Z) polymerization	DP of PBLA–PLys (Z)[a]	Mw/Mn[b]
PAsp14(DET)Lys48	1:25:50	DMF/20	DMF+CH_2Cl_2 (1:10)/40	14–48	1.16
PAsp36(DET)Lys50	1:45:50	DMSO/40	DMF+CH_2Cl_2 (1: 10)/40	36–50	1.13
PAsp66(DET)Lys47	1:80:50	DMF + CH_2Cl_2 (1:10)/40	DMF + CH_2Cl_2 (1:10)/40	66–47	1.28

[a] Determined from ^1H NMR.
[b] Determined from GPC.

80°C). In addition, other triblock copolymers, PEG-*b*-poly[*N*-(3-morpholylpropyl)aspartamide]-*b*-PLys (PEG–PAsp(APM)–PLys) and PEG-*b*-poly[*N*-(5-aminopentyl)aspartamide]-*b*-PLys (PEG–PAsp(DAP)–PLys), were similarly prepared by the aminolysis reaction of PEG–PBLA–PLys(Z) with 4-(3-aminopropyl)morpholine (20) and 1,5-diaminopentane (23), respectively. An ^{1}H NMR spectrum was measured with a JEOL EX300 spectrometer (JEOL, Tokyo, Japan). Chemical shifts are reported in ppm downfield from 3-(trimethylsilyl) propionic acid-d_4 sodium salt.

Cytotoxicity of PEG–PAsp(DET)–PLys Triblock Copolymer

A quantitative colorimetric assay with Cell Counting Kit-8 (Dojindo, Kumamoto, Japan) was carried out to evaluate cytotoxicity of block copolymers. This kit utilizes a colorimetric change from a soluble tetrazolium salt (WST-8) to WST-8 formazan by cytosolic dehydrogenases. Huh-7 cells (5,000 cells) were plated on 96-well plates and incubated overnight in 100 μL of DMEM containing 10% FBS. Then, the medium was changed to 100 μL of fresh medium containing 10% FBS and the polymers with various concentrations. After 24 h incubation, the medium was replaced with 100 μL of medium containing 10% FBS without polymers, followed by additional 24 h incubation. The medium was replaced with 120 μL of medium containing 10% FBS and 20 μL of Cell Counting Kit-8 solution, and then, incubated at 37°C for 3 h. The absorbance at 450 nm of the produced WST-8 formazan in each well was measured using a microplate reader (Model 680, Bio-rad). The cytotoxicity of block copolymers was estimated as a growth inhibitory concentration required for 50% reduction in cell population (IC50). The IC50 value of each block copolymer was calculated from a ratio of the obtained absorbance with the polymer to control without polymers. The results are presented as means and standard errors obtained from eight samples.

Preparation of PEG–PAsp(DET)–PLys/pDNA Polyplex Micelle

Each polymer was dissolved in 10 mM Tris–HCl (pH 7.4) buffer at a concentration of 2–5 mg/mL. These polymer solutions were then mixed with pDNA solution in 10 mM Tris–HCl (pH 7.4; final pDNA concentration: 33 μg/mL for *in vitro* assay and 100 μg/mL for *in vivo* assay) at varying mixing ratios.

Ethidium Bromide Exclusion Assay

Each polyplex micelle solution with 33 μg pDNA/mL, prepared by simply mixing pDNA and block copolymers at varying mixing ratios in 10 mM Tris–HCl (pH 7.4), was diluted to 10 μg pDNA/mL containing 2.5 μg EtBr/mL and 150 mM NaCl with the same buffer. The fluorescence intensity of the polyplex micelle solutions at λ=590 nm excited by UV laser (365 nm) was measured using a NanoDrop (ND-3300 Fluorospectrometer, Wilmington, DE, USA). The reference was set with 10 mM Tris–HCl (pH 7.4). The relative fluorescence intensity was calculated as follows:

$$F_r = (F_{sample} - F_0)/(F_{100} - F_0)$$

where F_{sample} is the fluorescence intensity of the micelle samples, F_{100} is that of the free pDNA, and F_0 is the background without pDNA. The results are presented as a mean and standard deviations (SD) obtained from three samples.

Dynamic Light Scattering and Zeta Potential Measurements

DLS and zeta potential measurements were performed using a Zetasizer nanoseries (Malvern Instruments Ltd., UK) at a detection angle of 173° and a temperature of 37°C. An He–Ne laser (λ=633 nm) was used as an incident beam. Polyplex solutions with various N^+/P ratios were prepared to a pDNA concentration of 33 μg/mL in 10 mM Tris–HCl (pH 7.4) buffer. The N^+/P ratio was defined as the molar ratio of protonated amino groups in block copolymers at pH 7.4 to phosphate groups in pDNA. The protonation degrees of lysine and Asp(DET) units at pH 7.4 were estimated to be 1.0 and 0.5, respectively, from the potentiometric titration results (13,24). In the DLS measurement, the sample solutions were injected into a small glass cuvette (volume: 12 μL), ZEN2112 (Malvern Instruments, Ltd.). The data obtained from the rate of decay in the photon correlation function were analyzed by the cumulant method, and the corresponding hydrodynamic diameter of the micelles was then calculated by the Stokes–Einstein equation (25). In the case of zeta potential measurement, the sample solutions were injected into folded capillary cells (Malvern Instruments, Ltd.). From the obtained electrophoretic mobility, the zeta potential was calculated by the Smoluchowski equation:

$$\zeta = 4\pi\eta\upsilon/\varepsilon$$

where η is the viscosity of the solvent, υ is the electrophoretic mobility, and ε is the dielectric constant of the solvent. The results are presented as a mean and SD obtained from three samples.

In Vitro Transfection (Luciferase Assay)

Huh-7 cells (20,000 cells) on 24-well culture plates were incubated with polyplex micelles containing 1 μg pDNA (Lys/Phosphate=2) in 400 μL of DMEM containing 10% FBS, followed by 24-h incubation and replacement with fresh medium. At 24 h post-incubation, the cells were washed with 400 μL of Dulbecco's PBS, and lysed with 200 μL of the cell culture lysis buffer (Promega). The luciferase activity of the lysates was evaluated from the photoluminescence intensity using the Luciferase Assay System and a Mithras LB 940 (Berthold Technologies). The obtained luciferase activity was normalized with the amount of proteins in the lysates determined by the Micro BCA™ Protein Assay Reagent Kit. The results are presented as means and standard errors obtained from four samples.

Cellular Uptake Study of Polyplex Micelles

pDNA was radioactively labeled with ^{32}P-dCTP using the Nick Translation System (Invitrogen, San Diego, CA, USA). Unincorporated nucleotides were removed using High Pure PCR Product Purification Kit (Roche Laboratories, Nutley, NJ, USA). After purification, 2 μg of labeled pDNA

was mixed with 400 μg of non-labeled pDNA. The polyplex micelle samples were prepared by mixing the radioactive pDNA solution with each polymer solution (Lys/Phosphate = 2 and 33 μg pDNA/mL). Huh-7 cells were seeded on 24-well culture plates in DMEM containing 10% FBS. After 24-h incubation, the cells were incubated for 24 h with 30 μL of the radioactive micelle solution (1 μg pDNA/well) in 400 μL of DMEM containing 10% FBS. The cells were then washed three times with Dulbecco's PBS and lysed with 400 μL of the cell culture lysis buffer. The lysates were mixed with 5 mL of scintillation cocktail, Ultima Gold (PerkinElmer, MA, USA), and the radioactivity of the mixtures was measured by a scintillation counter. The results are presented as means and standard errors obtained from four samples.

Intracellular Distribution of Cy5-labeled pDNA Evaluated Through Confocal Laser Scanning Microscope

pDNA was labeled with Cy5 using the Label IT Cy5 Labeling Kit according to the manufacturer's protocol. Huh-7 cells (50,000 cells) were seeded on a 35-mm glass base dish (Iwaki, Japan) and incubated overnight in 1 mL DMEM containing 10% FBS. After replacement of used medium with 1 mL of fresh medium, 90 μL of polyplex solution (Lys/Phosphate=2) containing 3 μg of Cy5-labeled pDNA was applied to the glass dish. After 24-h incubation, the medium was removed and the cells were washed three times with PBS. The intracellular distribution of each polyplex was observed by CLSM after staining acidic late endosomes and lysosomes with LysoTracker Green (Molecular Probes, Eugene, OR, USA) and nuclei with Hoechst 33342 (Dojindo Laboratories, Kumamoto, Japan). The CLSM observation was performed using LSM 510 (Carl Zeiss, Germany) with a ×63 objective lens (C-Apochromat, Carl Zeiss, Germany) at the excitation wavelengths of 488 nm (Ar laser), 633 nm (He–Ne laser), and 710 nm (MaiTai laser for 2-photon imaging) for LysoTracker Green (green), Cy5 (red), and Hoechst 33342 (blue), respectively.

In Vivo Enhanced Green Fluorescence Protein Expression in Subcutaneous Tumor Through Intravenous Injection of Polyplex Micelles

Human pancreatic adenocarcinoma cells (BxPC3) were grown in RPMI medium 1640 supplemented with 10% FBS. BALB/c nude mice (female, 5 weeks old) were obtained from Charles River Laboratories (Tokyo, Japan). All animal experimental protocols were performed in accordance with the Guide for the Care and Use of Laboratory Animals as stated by the NIH. BxPC3 cells (5×10^6 cells in 100 μL of PBS) were injected subcutaneously into the BALB/c nude mice and allowed to grow for 2–3 weeks to reach the proliferative phase. TβR-I inhibitor, dissolved to 5 mg/mL in DMSO and diluted by 100 μL of PBS, was intraperitoneally injected at 1 mg/kg 24 h before polyplex micelle administration. Polyplex micelles (Lys/Phosphate=2) containing EGFP gene in 200 μL of 10 mM HEPES buffer (pH 7.4) were intravenously injected through the tail vein at a dose of 20 μg pDNA/mouse. The mice were sacrificed 3 days after the injection. Tumors were excised, fixed with 10% formalin, and frozen in dry-iced acetone. The frozen samples were further sectioned at a 10-μm thickness in a cryostat. Immunostaining was carried out using anti-PECAM-1 antibody followed by Alexa647-conjugated secondary antibody for staining of vascular endothelial cells. The samples were observed by LSM 510 at excitation wavelengths of 488 and 633 nm for EGFP (green) and Alexa647 (red), respectively.

RESULTS

Preparation of PEG–PAsp(DET)–PLys Triblock Copolymer

A triblock copolymer of PEG, PBLA, and PLys(Z) (PEG–PBLA–PLys(Z)) as a precursor of the cationic triblock copolymer, PEG–PAsp(DET)–PLys, was synthesized by the two-step ring-opening polymerization of BLA–NCA (step 1) and Lys(Z)–NCA (step 2), initiated from the primary amine of PEG–NH_2 as shown in Fig. 1. In this way, a series of triblock copolymers with varying DPs of PBLA and PLys(Z) segments were prepared. As summarized in Table I, the obtained PEG–PBLA–PLys(Z)s were confirmed to have narrow Mw/Mn from the GPC, and the number of repeating units in PBLA and PLys(Z) segments was calculated from the peak intensity ratio of PBLA and PLys(Z) to PEG in the ^{1}H NMR spectra (data not shown). The conversion of flanking benzyl ester in the PBLA segment to *N*-(2-aminoethyl)-2-aminoethyl group was carried out by aminolysis reaction of PEG–PBLA–PLys(Z) with DET, followed by deprotection of the Z group of the PLys(Z) segment to obtain PEG–PAsp(DET)–PLys. The quantitative conversion of PBLA to PAsp(DET) and the complete deprotection of Z group were verified by ^{1}H NMR from the peak intensity ratio of the methylene protons in the *N*-(2-aminoethyl)-2-aminoethyl group ($H_2N(CH_2)_2NH(CH_2)_2NH$–, δ=3.1–3.5 ppm) to the β-methylene protons in the poly(aspartamide) (–CHCH_2CO–, δ=2.8 ppm) and the disappearance of the Z group peaks ($C_6H_5CH_2$–, δ=7.3 and 5 ppm), respectively, as typically seen in Fig. 2. The obtained PEG–PAsp(DET)–PLys was abbreviated as PAspX(DET)LysY, where X and Y represent the DP of the PAsp(DET) and PLys segments, respectively. Similarly, control diblock copolymers, PEG–PAsp(DET) and PEG–PLys, were abbreviated as PAspX(DET) and PLysY, respectively.

Cytotoxicity of PEG–PAsp(DET)–PLys Triblock Copolymer

The cytotoxicity of block copolymers, PEG–PAsp(DET), PEG–PLys, and PEG–PAsp(DET)–PLys, was compared and summarized as IC50 values in Table II. Obviously, PEG–PAsp(DET) showed much lower cytotoxicity than the others. The IC50 value of PAsp36(DET)Lys50 at the basis of polymer concentration (μM) was the similar level to that of PLys48, indicating that introduction of PAsp(DET) intermediate segment between PEG and PLys has negligible influence on the cytotoxicity of the block copolymer.

Formation of PEG–PAsp(DET)–PLys/pDNA Polyplex Micelles

Complex formation of pDNA with the triblock copolymer (PAsp36(DET)Lys50) was confirmed by EtBr exclusion assay. While EtBr molecules are known to emit strong fluorescence with their intercalation to DNA duplexes,

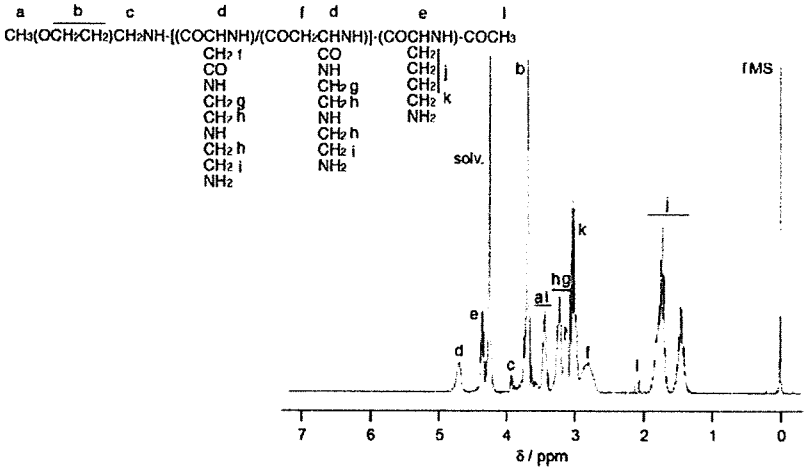

Fig. 2. ^{1}H NMR spectrum of the triblock copolymer, PAsp36(DET)Lys50. (Solvent, D_2O; temperature, 80°C; concentration, 10 mg/mL).

DNA condensation by cationic molecules inhibits such intercalation, resulting in decreased fluorescence. Accordingly, the measurement of the EtBr fluorescence allows the estimation of the process of pDNA condensation (26). The obtained fluorescence data are shown in Fig. 3a. The N/P ratio was defined as the residual molar ratio of total amino groups in the block copolymer to phosphate groups in the pDNA. The fluorescence change in PAsp36(DET)Lys50 seems to reach a plateau at an N/P ratio of 1.5. On the other hand, PLys48 and PAsp39(DET) as control diblock polycations reached plateaus at different N/P ratios; i.e., 1 for PLys48 and 2 for PAsp39(DET). In the plateau region, the fluorescence intensity was similar between PLys48 and PAsp36(DET)Lys50 possessing the PLys segment, while PAsp39(DET) showed higher fluorescence intensity than the others. This result suggests that the PLys segment may have higher ability of pDNA condensation than the PAsp(DET) segment to induce effective dye-exclusion. Then, the fluorescence data was replotted against the residual molar ratio of protonated amino groups to phosphate groups (N^+/P ratio; Fig. 3b). The protonation degree of Lys and Asp(DET) units at pH 7.4 was defined as 1.0 and 0.5, respectively, which were determined from potentiometric titration results of PEG–PLys (24) and PEG–PAsp(DET) diblock copolymers (13). Interestingly, in Fig. 3b, fluorescence profiles of all the samples showed similar trends, leveling off around the N^+/P ratio of 1, indicating that the protonated fraction of amino groups principally participates in the complexation with phosphate groups in the pDNA.

Table II. Growth Inhibitory Effects of the Block Copolymers Against Huh-7 Cells

	IC50		
Sample	Polymer concentration (μg/mL)	Polymer concentration (μM)	Amine concentration (μM)
PAsp68(DET)	>225	>7.35	>1,000
PLys48	26.1±1.4	1.2±0.1	57.0±3.1
PAsp36(DET)Lys50	29.5±0.8	0.9±0.04	114.4±4.9

Size and Zeta Potential of PEG–PAsp(DET)–PLys/pDNA Polyplex Micelles

The size and surface charge of gene vectors crucially affect their biological performance. Thus, these values of the polyplex micelles were determined by DLS and zeta potential measurements, respectively. As shown in Fig. 4a, the size of polyplex micelles gradually decreased with the N^+/P ratio, converging to the range of 60–80 nm in the region of $N^+/P>2$. The polyplex micelles from the triblock copolymer (PAsp36(DET)Lys50) were slightly smaller in size than those from the diblock copolymers (PAsp39(DET) and PLys48). As seen in Fig. 4b, all of the polyplex micelles showed almost neutral zeta potential at the N^+/P ratio of 1. Nevertheless, the micelles kept their initial size without any agglomeration even after overnight standing, as is consistent with the formation of a PEG palisade surrounding the polyplex core. Increasing the N^+/P ratio from 1 caused an increase in the zeta potential to a positive value, presumably due to the adsorption of excess block copolymers to the polyplex micelles as previously observed for PEG–P[Lys-*random*-Asp(DET)] block copolymer systems (19). The most prominent increase in the zeta potential with N^+/P was observed for the PAsp36(DET)PLys50 system, which may be explained by the decrease in PEG density of polyplex micelles due to the relative increase in the total length of cationic segments in the block copolymers; e.g., 39 for PAsp39(DET), 48 for PLys48, and 86 for PAsp36(DET)Lys50. Providing the micelles have the same compositional N^+/P ratio at a given feeding N^+/P ratio, the density of PEG should decrease with an increase in the length of the cationic segment. In this regard, the values of the zeta potential were compared between PAsp36(DET)Lys50 triblock micelles and PLys109 diblock (PEG–PLys) micelles having longer-length cationic PLys segments (Fig. 4c). Obviously, the PAsp36(DET)Lys50 micelles still had higher zeta potential than the PLys109 micelles. This finding indicates that the zeta potential of polyplex micelles in the region of excess block copolymers is not simply correlated to the length of the cationic segment, and that the difference in the chemical structure of cationic amino acid residues, in this case Lys and PAsp(DET), crucially affects the composition and structure of the polyplex micelles.

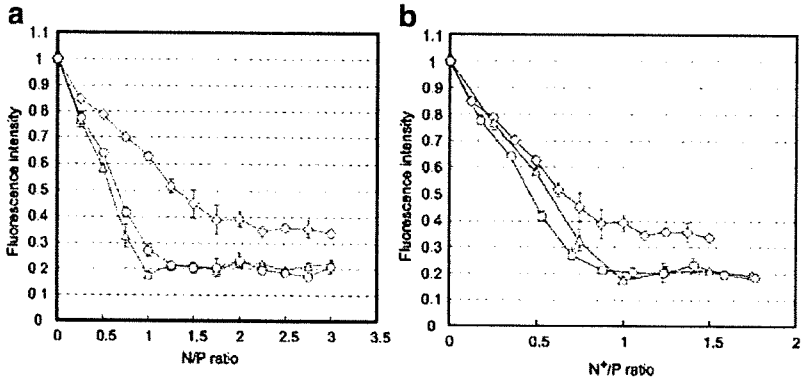

Fig. 3. EtBr dye exclusion assay on the polyplex micelles with varying compositions prepared from PAsp39(DET) (*diamonds*), PLys48 (*triangles*), and PAsp36(DET)Lys50 (*circles*; pDNA concentration, 10 μg/mL; EtBr concentration, 2.5 μg/mL; Temperature, 25°C; Medium, 10 mM Tris–HCl (pH 7.4) containing 150 mM NaCl). **a** The relationship with the N/P ratio, i.e., the residual molar ratio of amino groups in the polymer to phosphate groups in the pDNA. **b** The relationship with the N^+/P ratio, the residual molar ratio of protonated amino groups in the polymer to phosphate groups in pDNA at pH 7.4. Results were expressed as mean±SD (n=3).

To verify the influence of the order of the cationic components in the triblock copolymer, the zeta potential of the polyplex micelles from PEG–PLys–PAsp(DET) (the DPs of PLys and PAsp(DET) were 48 and 33, respectively) was also measured. As seen in Fig. 4d, the polyplex micelles from PLys48Asp33(DET) showed the similar level of zeta potential to those from PLys48. This indicates that PAsp (DET) aligned as an intermediate segment contributes to the higher zeta potential of the PAsp36(DET)Lys50 (Fig. 4b–d).

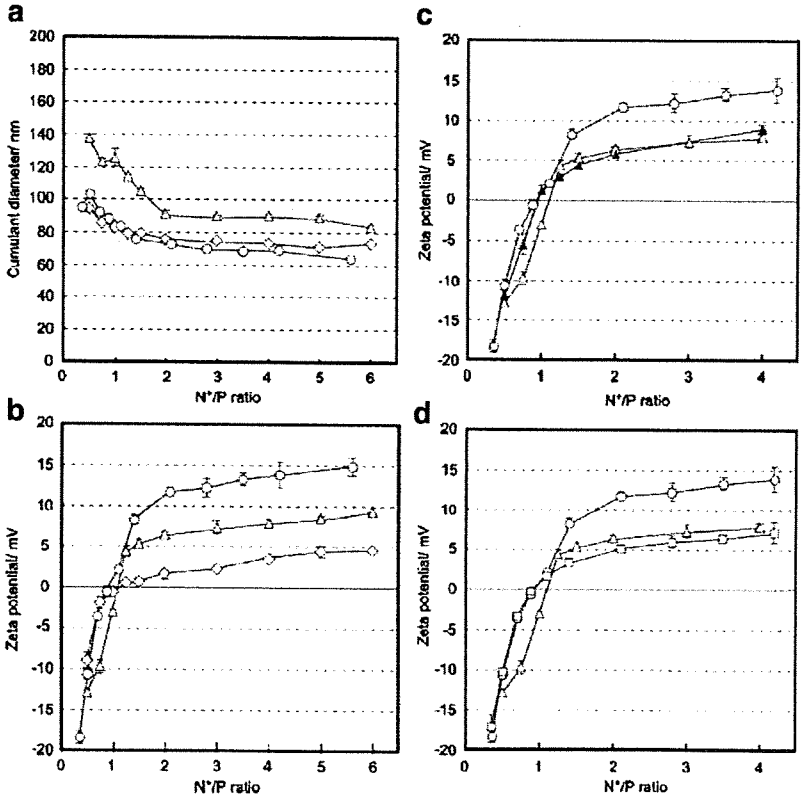

Fig. 4. Size and zeta potential of the polyplex micelles. **a** Size. **b**, **c**, **d** Zeta potential. PAsp39(DET); *diamonds*. PLys48; *empty triangles*. PLys109; *filled triangles*. PAsp36(DET) Lys50; *circles*. PLys48Asp33(DET); *squares*. (pDNA concentration, 33.3 μg/mL; Temperature, 37°C). Results were expressed as mean±SD (n=3).

In Vitro Transfection with Polyplex Micelles Prepared from Triblock Copolymer with Varying Polycations as an Intermediate Segment

Polyplex micelles were prepared from triblock copolymers with different polycation segments aligned between PEG and PLys segments and were subjected to a luciferase assay against Huh-7 cells in order to explore whether the change in the chemical composition of the intermediate polycation layer affects the transfection efficiency. As will be addressed in "DISCUSSION" section, the polyplex micelles from triblock copolymer is likely to take three layered structure at least in the region of excess polycation ($N^+/P>1$): the outer layer of PEG, the middle layer of buffering polycation, and the inner core of condensed PLys/pDNA polyplex (20). PLys segment, which is almost fully charged at physiological pH, is assumed to principally participate in the polyplex formation, keeping the intermediate polycation as free form in the middle layer of the micelles. Thus, it may be reasonable to compare the transfection efficiency of these polyplex micelles from the triblock copolymers with different intermediate segments at the fixed Lys/Phosphate ratio instead of N^+/P ratio, because the latter includes the contribution from the charged amino groups that may not directly participate in the polyplex formation. Here, the Lys/Phosphate ratio is fixed to 2 because the previous study revealed that pDNA condensation is completed at this ratio, exerting the optimal transfection efficiency (26).

The DPs of the intermediate polycations (PAsp(DAP), PAsp(APM), and PAsp(DET) as illustrated in Fig. 5a and the PLys in the triblock copolymers were fixed to 36 and 50, respectively, in this experiment. Fig. 5b clearly shows that the luciferase activity strongly depends on the structure of the intermediate polycation segments in the block copolymers. The polyplex micelles from the PAsp36(DAP)Lys50 showed a similar level of luciferase expression as those from the PLys48, indicating that the introduction of PAsp(DAP) segments with a similar pKa value, 9.9, to PLys had a negligible effect on the transfection efficacy. In line with our previous results (20), the polyplex micelles from the PAsp36(APM)Lys50 revealed some improvements in transfection efficacy compared to the PLys48 micelles. Notably, the highest transfection efficacy was achieved by polyplex micelles from the PAsp36(DET)Lys50, which showed tenfold higher luciferase activity than that from PLys48. On the other hand, the polyplex micelles from PEG–PLys–PAsp(DET) (the DPs of PLys and PAsp(DET) were 48 and 33, respectively), where the order of cationic segments between PAsp(DET) and PLys was inversed in the triblock copolymer, exhibited substantially decreased transfection efficacy compared with those from PAsp36(DET)Lys50.

The effect of the length of the cationic segments on the transfection efficacy was then studied in detail as seen in Fig. 5c. There was observed a critical increase in the transfection efficacy for PEG–PLys systems between the PLys20 and PLys48. It should be noted that one order of magnitude higher transfection was always obtained for the triblock systems compared to the diblock systems having similar total DPs of polycation segments (PLys71 *vs.* PAsp36(DET)Lys50 and PLys109 *vs.* PAsp66(DET)Lys47), supporting the result described in the preceding paragraph that the PAsp(DET) segment aligned as the intermediate segment plays a substantial role in the enhanced transfection.

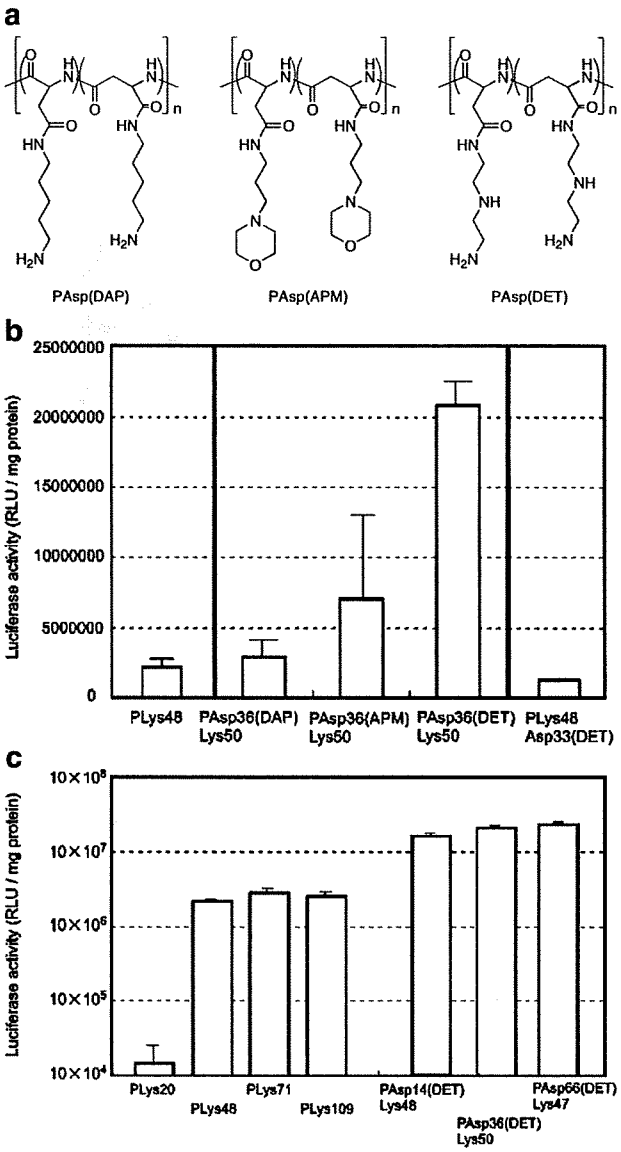

Fig. 5. Transfection efficacy of the polyplex micelles against Huh-7 cells (Luciferase assay). **a** Chemical structures of PAsp(DAP), PAsp (APM), and PAsp(DET) as the intermediate segment in the triblock copolymers. **b** Transfection efficacy of the polyplex micelles from PLys48, a series of triblock copolymers (PAsp36(R)Lys50) with varying intermediate segments (PEG–PAsp(DAP)–PLys, PEG–PAsp(APM)–PLys, and PEG–PAsp(DET)–PLys), and a triblock copolymer with the reversed order of the cationic segments, PLys48Asp33(DET). **c** Effect of the length of the cationic segments in di- or triblock copolymers on transfection efficacy. All the micelle samples were prepared at a Lys/Phosphate= 2 and applied for the transfection (pDNA concentration, 2.3 μg/mL).

Cellular Uptake and Intracellular Distribution of PEG–PAsp (DET)–PLys/pDNA Polyplex Micelles

From the results of luciferase assay, a PAsp(DET) segment integrated into the middle of the triblock copolymers was confirmed to improve the transfection activity of the polyplex micelles, consistent with the hypothesis of facilitated

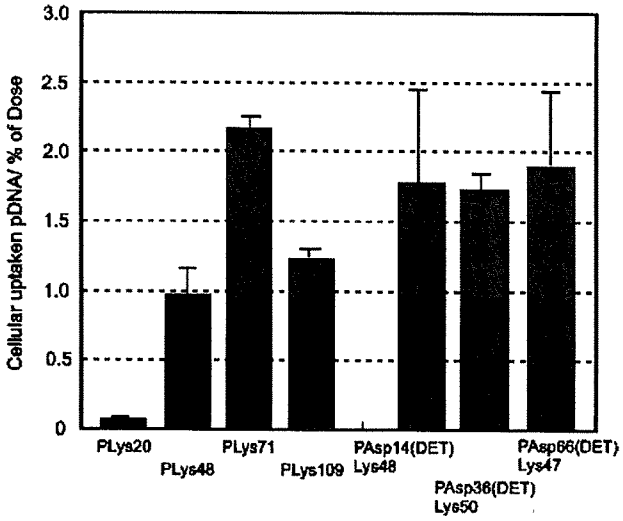

Fig. 6. Uptake into Huh-7 cells of ^{32}P-labeled pDNA in the polyplex micelles. All the micelle samples were prepared at a Lys/Phosphate= 2 and applied for the experiments (pDNA concentration, 2.3 μg/mL).

endosomal escape. Nevertheless, there is also a possibility that the higher zeta potential of PEG–PAsp(DET)–PLys micelles compared to other PEGylated systems (Fig. 4b,c) may facilitate their cellular uptake, leading to the improved transfection. Hence, a cellular uptake study was carried out using ^{32}P-labeled pDNA under a similar condition to the luciferase assay (Fig. 6). PLys20 micelle exhibited significantly lower uptake than those of other micelles, corresponding to its low transfection efficacy as shown in Fig. 5c. All of the micelles prepared from the diblock and triblock copolymers composed of PLys segments with DPs over 47 showed similar levels of cellular uptake. There was no significant difference in the efficacy of cellular uptake between the micelles with and without a PAsp(DET) segment as the middle block, excluding the facilitated cellular uptake as the reason for the improved transfection observed for the polyplex micelles from the triblock copolymers.

Then, intracellular distribution of the polyplex micelles from PLys48 and PAsp36(DET)Lys50 was observed by CLSM to estimate the efficacy of endosomal escape of the polyplex micelles. The pDNA, nuclei, and late endosomes/lysosomes were simultaneously stained with Cy5 (red), Hoechst33342 (blue), and LysoTracker (green), respectively. The Cy5-pDNA introduced into the PLys48 micelles without a PAsp(DET) segment was observed as discrete dots partially colocalizing with the late endosome/lysosome markers (yellow spots) 24 h after the addition of the polyplex micelles (Fig. 7a), indicating that the PLys48 polyplex micelles were segregated in intracellular compartments including late endosomes/lysosomes. In contrast, the Cy5-pDNA in PAsp36 (DET)Lys50 polyplex micelles spread more clearly in the cytoplasmic region (Fig. 7b), demonstrating that effective endosomal escape had occurred. These results strongly support that the PAsp(DET) segment plays a crucial role in facilitating the endosomal escape of the polyplex micelles.

In Vivo Transfection by PEG–PAsp(DET)–PLys/pDNA Polyplex Micelle by Intravenous Administration

The transfection ability of the PAsp36(DET)Lys50 polyplex micelles by systemic administration was estimated from EGFP expression in subcutaneously xenografted human pancreatic adenocarcinoma, BxPC3. As previously reported, this tumor tissue has a poorly differentiated histology with a certain number of blood vessels and thick fibrotic tissue in the stroma (21); i.e., closely resembling the histology of certain intractable tumors observed in clinical specimens. The fluorescence microscopy of the sectioned xenografted tumors was obtained with immunostaining of tumor vasculature by PECAM-1 (red), and nuclear counter staining (blue; Fig. 8a). Apparently, the BxPC3 tumors were shown to have wide stromal regions (region S) surrounding nests of tumor cells (region T) and blood vasculature (region V). Fig. 8b shows the image of EGFP expression (green) in the BxPC3 tumor tissue receiving intravenous injection of the PAsp36(DET) Lys50 polyplex micelles incorporating pDNA coding for EGFP. The EGFP expression was evident, yet the intensity was very weak. Worth noting is that TβR-I inhibitor, which has been found to facilitate the accumulation of macromolecular drugs in tumor tissues (21), drastically improved the EGFP expression by the PAsp36(DET)Lys50 polyplex micelles (Fig. 8c). Note that the PAsp36(DET)Lys50 polyplex

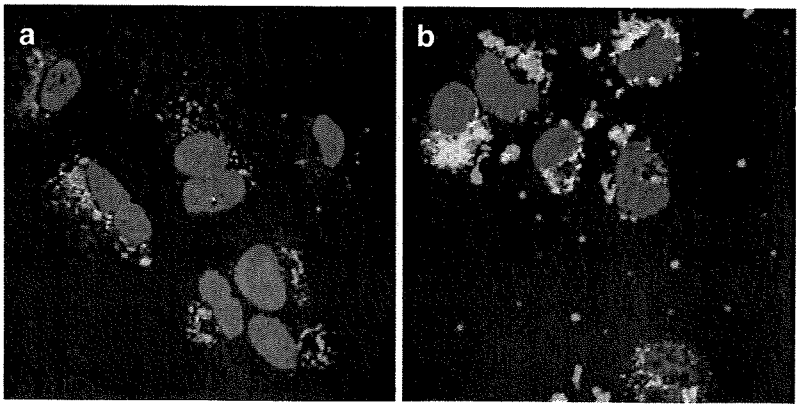

Fig. 7. Intracellular distribution of the PLys48 (**a**) and PAsp36(DET)Lys50 (**b**) micelles prepared at a Lys/Phosphate=2. The pDNA was labeled with Cy5 (*red*), and the late endosomes/lysosomes and the nucleus were stained with LysoTracker (*green*) and Hoechst33342 (*blue*), respectively. (pDNA concentration, 2.8 μg/mL).

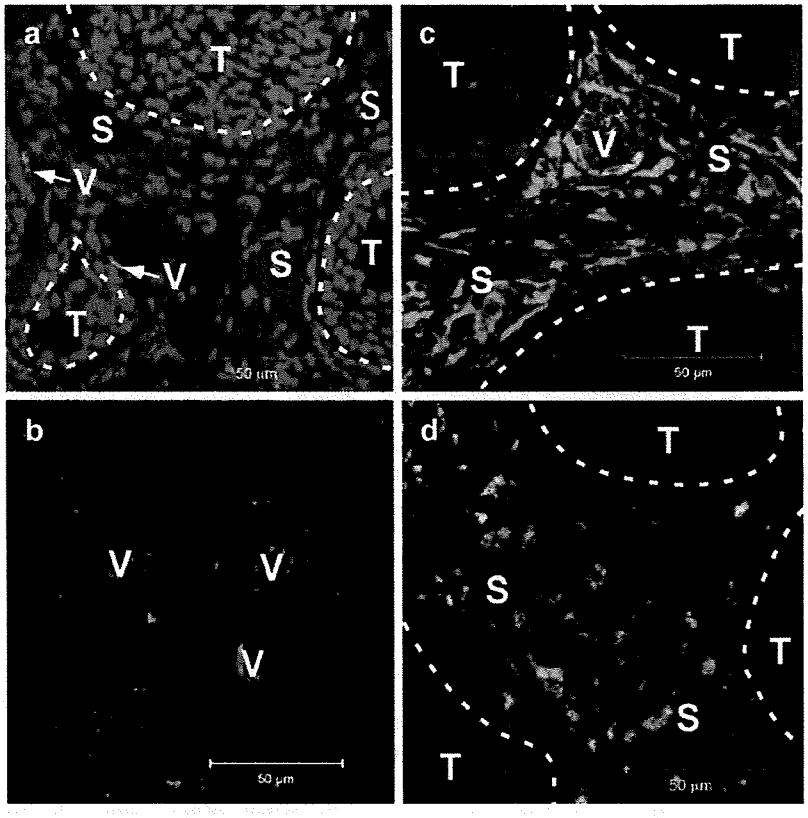

Fig. 8. EGFP transfection into subcutaneous tumors of pancreatic adenocarcinoma cells, BxPC3, *via* systemic route. Each micelle sample was prepared at a Lys/Phosphate=2, and intravenously injected through the tail veins of the mice (20 μg pDNA/mouse). **a** Histology of BxPC3 xenograft as a model of poorly differentiated pancreatic tumor tissue. *Blue*: nucleus stained with Hoechst 33342, *red*: PECAM-1 as an endothelial marker stained with Alexa647-conjugated secondary antibody against anti-PECAM-1 antibody (regions *T*, *S*, and *V* indicate nests of tumor cells in tumor tissues, thick fibrotic tissue in the stroma, and blood vasculature, respectively). **b** EGFP expression by PAsp36(DET)Lys50 polyplex micelle without TβR-I inhibitor; **c** EGFP expression by PAsp36(DET)Lys50 polyplex micelle with TβR-I inhibitor; **d** EGFP expression by PLys71 polyplex micelles with TβR-I inhibitor.

micelles in combination with TβR-I inhibitor did not show detectable EGFP expression in the liver and lung under the tested conditions (data not shown). Fig. 8d shows the result obtained for the PLys71 polyplex micelles with TβR-I inhibitor. Obviously, the EGFP expression by the PAsp36 (DET)Lys50 polyplex micelles was much more remarkable than that with the PLys71 polyplex micelles, suggesting that the integration of the PAsp(DET) segment into the polyplex micelles is effective even in the transfection by systemic administration. Detailed observation of the fluorescence images revealed that the EGFP expression by the polyplex micelles was located mainly around PECAM-1-positive vascular endothelial cells. As typically shown in Fig. 8a, the tumor stroma grows around the nests of tumor cells in BxPC3 subcutaneous xenografts, and blood vasculature exists inside the stroma. Therefore, a major part of the EGFP expression in the BxPC3 tumor by PAsp36(DET)Lys50 polyplex micelles was not from BxPC3 cells *per se*, but from cells in the stroma including vascular endothelial cells and fibroblasts.

DISCUSSION

In the present study, polyplex micelles with an endosomal escape layer were prepared from a triblock copolymer for the purpose of transfection into solid tumors through systemic routes. The triblock copolymer was composed of three tandemly aligned functional segments as follows: PEG for biocompatibility, PAsp(DET) for efficient endosomal escape, and PLys for pDNA condensation. A series of triblock copolymers, PEG–PAsp(DET)–PLys, with the DP of PLys of approximately 50, was synthesized and used for the preparation of the polyplex micelles, according to the previous results that a DP of approximately 48 was needed for effective transfection with polyplex micelles from PEG–PLys as shown in Fig. 5c as well as for the prolonged circulation of intact pDNA in the blood stream (10). The triblock copolymer, PAsp36(DET)Lys50, as well as the diblock PEG–PLys, PLys48, effectively condensed pDNA to form a polyplex micelle (Fig. 3). The obtained polyplex micelles

from the triblock copolymer were around 80 nm at an N^+/P ratio of 1 or greater (Fig. 4a), thereby having the potential ability to accumulate in tumors through the enhanced permeability and retention (EPR) effect (27). Also, the zeta potential measurement indicated that the excess positive charge of the polyplex micelle from the triblock copolymer was reasonably shielded by a PEG palisade surrounding the polyplex core (Fig. 4b). It should be noted that PEGylation of polyplexes facilitates their penetration into tumor spheroids (15, 16). Hence, the PEG palisade of polyplex micelles from the triblock copolymer may contribute to promoting their permeation into the tumor tissue *via* extravasation as well as to extending their plasma half-life through a steric stabilization effect, leading to appreciable gene expression in the subcutaneous pancreatic tumor tissue as seen in Fig. 8. Note that the xenografted pancreatic tumor, BxPC3, was chosen as our target in this study. Since pancreatic tumors are representative of intractable tumors, which are difficult to treat by conventional therapy, they are an appropriate target for the development of new strategies including gene therapy. However, it is also difficult to deliver exogenous genes to such tumor tissue by gene carriers through an EPR effect, presumably due to their thick fibrotic and hypovascular characteristics. In this regard, the combined use of TβR-I inhibitor, which has been found to decrease pericyte coverage of the endothelium specifically in tumor neovasculature (21), is available for the enhancement of accumulation of nanocarriers of 60–100 nm diameter into the solid tumor. Indeed, the EGFP expression by the polyplex micelles from PAsp36(DET)Lys50 was substantially improved by the intraperitoneal injection of TβR-I inhibitor (Fig. 8b,c). The size of the polyplex micelle was approximately 80 nm, thereby making it suitable for combination with TβR-I inhibitor. As far as we know, this is the first example of effective gene expression in BxPC3 tumors with thick fibrotic and hypovascular characteristics *via* systemic administration of non-viral vectors. In addition, detailed observation of the fluorescence images from sectioned xenografted tumors revealed that the EGFP expression by the PAsp36(DET)Lys50 polyplex micelle combined with TβR-I inhibitor was located mainly around the blood vasculature (Fig. 8c), suggesting that the transfection with the polyplex micelle was not effective for the tumor cells *per se*, but for the cells in the tumor stroma, including vascular endothelial cells and fibroblasts. These results suggest that the penetration of polyplex micelles into tumor microenvironments may still be a major challenge, even with the aid of TβR-I inhibitor for successful systemic transfection directly to the BxPC3 tumor cells. In this regard, for the gene therapy of pancreatic adenocarcinoma with thick fibrotic tissues, the approach of treating the tissues surrounding the nests of tumor cells would be more realistic than that directly targeting tumor cells *per se*, e.g., with a tumor suppressor gene to induce apoptosis. Antiangiogenic gene therapy is one of the typical "indirect" approaches to treating fibrotic tumors, and research in this direction on combination treatment using polyplex micelles and TβR-I inhibitor is now ongoing in our laboratory.

The contribution of the PAsp(DET) segment in the triblock copolymer to improved transfection without increased cytotoxicity was obvious from the results of both *in vitro* and *in vivo* transfection studies (Figs. 5, 8, and Table II). It should be noted that there is no significant difference in cellular uptake between the polyplex micelles from the triblock and diblock copolymers (Fig. 6), even though the former revealed almost one order of magnitude higher transfection efficacy than the latter. This result suggests that the major cause for the facilitated transfection with the polyplex micelles from the triblock copolymer may be in the intracellular stage. Indeed, the CLSM observation clearly revealed the facilitated endosomal escape of pDNA associated with the polyplex micelles from the triblock copolymer (Fig. 7), indicating the availability of PAsp(DET) as an endosomal escape element. PAsp(DET) is likely to form the middle layer between the PEG shell and the PLys/pDNA polyplex core in the micelles, because PLys with higher affinity to pDNA than PAsp(DET) is assumed to undergo preferential condensation of pDNA, relegating the PAsp (DET) segment to the boundary with the PEG layer. Increased freedom of PLys as an outer block with a free chain-end may also contribute to the preferential complexation with pDNA. Note that a similar three-layered structure was previously proposed by us for polyplex micelles prepared from PEG–PAsp(APM)–PLys based on the results of ^{1}H-NMR spectroscopy (20). The appreciably higher zeta potential of PAsp36(DET)Lys50 micelles in the region at an N^+/P ratio of 1 or greater is consistent with the formation of a cationic middle layer (Fig. 4b,c) that is not completely shielded by the outer PEG layer. Thus, the PAsp(DET) placed in the middle layer of polyplex micelles should exert endosomal escape ability for efficient transfection through strong buffering and/or a membrane-destabilizing effect based on the unique two-step protonation behavior of the 1,2-diaminoethane unit (13,15). On the other hand, as seen in Fig. 5b, the one order of magnitude lower transfection efficacy obtained by reversing the order of PLys and PAsp (DET) segments in the triblock copolymer is interesting. It is reasonable to consider that arrangement of the PLys segment, with its strong condensing power against pDNA, as the intermediate segment of the triblock copolymer may allow the PAsp(DET) segment to become embedded in the core of the polyplex micelles, resulting in the loss of buffering and/or membrane-destabilizing capacity. The zeta potential of the PEG–PLys–PAsp(DET) systems similar to that of the PEG–PLys systems also supports the disappearance of the intermediate buffering layer in the polyplex micelles from PEG–PLys–PAsp(DET) with the reversed order of the cationic segments (Fig. 4d).

CONCLUSION

For the achievement of systemic gene delivery to solid tumors with appreciable transfection efficacy, gene carriers are required to exert integrated functions including a stealth property in the blood stream to deliver intact pDNA into tumor tissues and permeate target cells with smooth translocation from endosomal compartments into the cytoplasm, subsequently releasing the pDNA to induce effective transcription. In the present study, to develop a gene carrier with such integrated functions, three segments with distinctive functions; i.e., PEG for biocompatibility, PAsp(DET) for endosomal escape, and PLys for pDNA condensation, were tandemly aligned in a polymer strand to form three-layered

polyplex micelles. The obtained micelles showed one order of magnitude higher transfection efficacy against Huh-7, compared to the micelles from the PEG–PLys diblock copolymer without any segments exerting an endosomal escape function. Notably, the polyplex micelle from the triblock copolymer achieved clear *in vivo* transfection of the EGFP gene in fibrotic pancreatic adenocarcinoma, BxPC3, through systemic administration. It should be emphasized that the EGFP expression in the pancreatic tumor was drastically enhanced by the intraperitoneal injection of TβR-I inhibitor prior to the micelle injection, and thus, the potential for combined therapy using polyplex micelles and TβR-I inhibitor for systemic transfection to solid tumors was clearly evidenced. Furthermore, detailed observation of the immunostained tumor tissues revealed that the EGFP expression by the triblock copolymer micelles was located mainly in the stromal tissues surrounding the nests of tumor cells. These results suggest that the triblock micelle is quite promising for fibrotic tumor treatments by the approach of transfecting the tissues surrounding tumor cells, including fibroblasts and endothelial cells, to express proteins inhibiting tumor angiogenesis.

ACKNOWLEDGEMENTS

This work was financially supported by the Core Research Program for Evolutional Science and Technology (CREST) from the Japan Science and Technology Corporation (JST) as well as by Special Coordination Funds for Promoting Science and Technology from the Ministry of Education, Culture, Sports, Science and Technology of Japan (MEXT).

REFERENCES

1. Wiley (2007) Gene Therapy Clinical Trials Worldwide, provided by the *J. Gene Med.* http://www.wiley.co.uk/genetherapy/clinical/ (accessed 17/01/08)
2. D. W. Pack, A. S. Hoffman, S. Pun, and P. S. Stayton. Design and development of polymers for gene delivery. *Nat. Rev. Drug Discov.* **4**:581–593 (2005) doi:10.1038/nrd1775.
3. E. Mastrobattista, M. A. E. M. van der Aa, W. E. Hennink, and D. J. A. Crommelin. Artificial viruses: a nanotechnological approach to gene delivery. *Nat. Rev. Drug Discov.* **5**:115–121 (2006) doi:10.1038/nrd1960.
4. E. Wagner. Strategies to improve DNA polyplexes for *in vivo* gene transfer: Will "artificial viruses" be the answer? *Pharm. Res.* **21**:8–14 (2004) doi:10.1023/B:PHAM.0000012146.04068.56.
5. Y. Kakizawa, and K. Kataoka. Block copolymer micelles for delivery of gene and related compounds. *Adv. Drug Deliv. Rev.* **54**:203–222 (2002) doi:10.1016/S0169-409X(02)00017-0.
6. S. Katayose, and K. Kataoka. Water-soluble polyion complex associates of DNA and poly(ethylene glycol)-poly(L-lysine) block copolymer. *Bioconjugate Chem.* **8**:702–707 (1997) doi:10.1021/bc9701306.
7. M. A. Wolfert, E. H. Schacht, V. Toncheva, K. Ulbrich, O. Nazarova, and L. W. Seymour. Characterization of vectors for gene therapy formed by self-assembly of DNA with synthetic block co-polymers. *Hum. Gene. Ther.* **10**:2123–2133 (1996) doi:10.1089/hum.1996.7.17-2123.
8. Y. H. Choi, F. Liu, J. Kim, Y. K. Choi, J. S. Park, and S. W. Kim. Polyethylene glycol-grafted poly-L-lysine as polymeric gene carrier. *J. Control. Release.* **54**:39–48 (1998) doi:10.1016/S0168-3659(97)00174-0.
9. K. Itaka, A. Harada, K. Nakamura, H. Kawaguchi, and K. Kataoka. Evaluation by fluorescence resonance energy transfer of the stability of nonviral gene delivery vectors under physiological conditions. *Biomacromolecules.* **3**:841–845 (2002) doi:10.1021/bm025527d.
10. M. Harada-Shiba, K. Yamauchi, A. Harada, I. Takamisawa, K. Shimokado, and K. Kataoka. Polyion complex micelles as a vector in gene therapy—pharmacokinetics and *in vivo* gene transfer. *Gene. Ther.* **9**:407–414 (2002) doi:10.1038/sj.gt.3301665.
11. O. Boussif, F. Lezoualc'h, M. A. Zanta, M. D. Mergny, D. Scherman, B. Demeneix, and J. Behr. A versatile vector for gene and oligonucleotide transfer into cells in culture and *in-vivo* polyethylenimine. *Proc. Natl. Acad. Sci. U. S. A.* **92**:7297–7301 (1995) doi:10.1073/pnas.92.16.7297.
12. M. Neu, D. Fischer, and T. Kissel. Recent advances in rational gene transfer vector design based on poly(ethylenimine) and its derivatives. *J. Gene Med.* **7**:992–1009 (2005) doi:10.1002/jgm.773.
13. N. Kanayama, S. Fukushima, N. Nishiyama, K. Itaka, W.-D. Jang, K. Miyata, Y. Yamasaki, U. Chung, and K. Kataoka. A PEG-based biocompatible block catiomer with high buffering capacity for the construction of polyplex micelles showing efficient gene transfer toward primary cells. *Chem. Med. Chem.* **1**:439–444 (2006) doi:10.1002/cmdc.200600008.
14. K. Masago, K. Itaka, N. Nishiyama, U. Chung, and K. Kataoka. Gene delivery with biocompatible cationic polymer: pharmacogenomic analysis on cell bioactivity. *Biomaterials.* **28**:5169–5175 (2007) doi:10.1016/j.biomaterials.2007.07.019.
15. M. Han, Y. Bae, N. Nishiyama, K. Miyata, M. Oba, and K. Kataoka. Transfection study using multicellular tumor spheroids for screening non-viral polymeric gene vectors with low cytotoxicity and high transfection efficiencies. *J. Control Release.* **121**:38–48 (2007a) doi:10.1016/j.jconrel.2007.05.012.
16. M. Han, Y. Bae, N. Nishiyama, and K. Kataoka. Gene delivery with poly(amino acid)-based block catiomer polyplex micelles against multicellular tumor spheroid. *Abstracts of 13th International Symposium on Recent Advances in Drug Delivery Systems*, Salt Lake City, UT, (2007b), pp. 128.
17. D. Akagi, M. Oba, H. Koyama, N. Nishiyama, S. Fukushima, T. Miyata, H. Nagawa, and K. Kataoka. Biocompatible micellar nanovectors achieve efficient gene transfer to vascular lesions without cytotoxicity and thrombus formation. *Gene. Ther.* **14**:1029–1038 (2007) doi:10.1038/sj.gt.3302945.
18. K. Itaka, S. Ohba, K. Miyata, H. Kawaguchi, K. Nakamura, T. Takato, U. Chung, and K. Kataoka. Bone regeneration by regulated *in vivo* gene transfer using biocompatible polyplex nanomicelles. *Mol. Ther.* **15**:1655–1662 (2007) doi:10.1038/sj.mt.6300218.
19. K. Miyata, S. Fukushima, N. Nishiyama, Y. Yamasaki, and K. Kataoka. PEG-based block catiomers possessing DNA anchoring and endosomal escaping functions to form polyplex micelles with improved stability and high transfection efficacy. *J. Control Release.* **122**:252–260 (2007) doi:10.1016/j.jconrel.2007.06.020.
20. S. Fukushima, K. Miyata, N. Nishiyama, N. Kanayama, Y. Yamasaki, and K. Kataoka. PEGylated polyplex micelles from triblock catiomers with spatially ordered layering of condensed pDNA and buffering units for enhanced intracellular gene delivery. *J. Am. Chem. Soc.* **127**:2810–2811 (2005) doi:10.1021/ja0440506.
21. M. R. Kano, Y. Bae, C. Iwata, Y. Morishita, M. Yashiro, M. Oka, T. Fujii, A. Komuro, K. Kiyono, M. Kamiishi, K. Hirakawa, Y. Ouchi, N. Nishiyama, K. Kataoka, and K. Miyazono. Improvement of cancer-targeting therapy, using nanocarriers for intractable solid tumors by inhibition of TGF-beta signaling. *Proc. Natl. Acad. Sci. U. S. A.* **104**:3460–3465 (2007) doi:10.1073/pnas.0611660104.
22. W. H. Daly, and D. Poche. The preparation of *N*-carboxyanhydrides of alpha-amino-acids using bis(trichloromethyl)carbonate. *Tetrahedron Lett.* **29**:5859–5862 (1988) doi:10.1016/S0040-4039(00)82209-1.
23. A. Koide, A. Kishimura, K. Osada, W. -D. Jang, Y. Yamasaki, and K. Kataoka. Semipermeable polymer vesicle (PICsome) self-assembled in aqueous medium from a pair of oppositely charged block copolymers: physiologically stable micro-/nanocontainers of water-soluble macromolecules. *J. Am. Chem. Soc.* **128**:5988–5989 (2006) doi:10.1021/ja057993r.
24. A. Harada, S. Cammas, and K. Kataoka. Stabilized α-helix structure of poly(L-lysine)-block-poly(ethylene glycol) in aque-

ous medium through supramolecular assembly. *Macromolecules.* **29**:6183–6188 (1996) doi:10.1021/ma960487p.
25. A. Harada, and K. Kataoka. Formation of polyion complex micelles in an aqueous milieu from a pair of oppositely-charged block copolymers with poly(ethylene glycol) segments. *Macromolecules.* **28**:5294–5299 (1995) doi:10.1021/ma00119a019.
26. K. Itaka, K. Yamauchi, A. Harada, K. Nakamura, H. Kawaguchi, and K. Kataoka. Polyion complex micelles from plasmid DNA and poly(ethylene glycol)-poly(L-lysine) block copolymer as serum-tolerable polyplex system: physicochemical properties of micelles relevant to gene transfection efficiency. *Biomaterials.* **24**:4495–4506 (2003) doi:10.1016/S0142-9612(03)00347-8.
27. Y. Matsumura, and H. Maeda. A new concept for macromolecular therapeutics in cancer chemotherapy: mechanism of tumoritropic accumulation of proteins and the antitumor agent SMANCS. *Cancer Res.* **46**:6387–6392 (1986).